Synthesis, Structure, Electronic, Redox, and Magnetic Properties of a New Mixed-Valent Mn-Oxo Cluster: $[Mn_2^{III,IV}O_2(N,N\text{bispicen})_2]^{3+}$ (*N*,*N*bispicen = *N*,*N*-bis(2-pyridylmethyl)-1,2-diaminoethane)

Olivier Horner[a,b], Marie-France Charlot[a], Alain Boussac[b], Elodie Anxolabéhère-Mallart[a], Lyuba Tchertanov[c], Jean Guilhem[c], and Jean-Jacques Girerd*[a]

Laboratoire de Chimie Inorganique, URA CNRS 420, Université Paris-Sud[a],
F-91405 Orsay, France

Section de Bioenergétique, URA CNRS 2096, CEA Saclay[b],
F-91191 Gif-sur-Yvette, France

Laboratoire de Cristallochimie, Institut de Chimie des Substances Naturelles UPR CNRS 2301[c],
F-91198 Gif-sur-Yvette, France

Received December 8, 1997

Keywords: Manganese / EPR spectroscopy / Spectroelectrochemistry / Mixed-valent compounds / Tripodal ligands

The synthesis and structural characterization of the novel $[Mn^{III,IV}{}_2O_2(N,N\text{bispicen})_2](ClO_4)_3{\cdot}CH_3CN$ complex employing the tetradentate ligand *N*,*N*bispicen = *N*,*N*-bis(2-pyridylmethyl)-1,2-diaminoethane are reported. Magnetic properties were determined and show that the ground state is a spin doublet. This can be quantitatively interpreted by antiferromagnetic coupling between a Mn(III) high spin and a Mn(IV) ($J = -316\ cm^{-1}$). The 16 line solution EPR spectrum exhibits an unusual splitting in the low field resonances.The following rhombic tensors were needed to simulate the EPR spectrum: $|A_{1x}| = 160\ 10^{-4}\ cm^{-1}$, $|A_{1y}| = 144\ 10^{-4}\ cm^{-1}$, $|A_{1z}| = 109\ 10^{-4}\ cm^{-1}$, $|A_{2x}| = 69\ 10^{-4}\ cm^{-1}$, $|A_{2y}| = 72\ 10^{-4}\ cm^{-1}$, $|A_{2z}| = 75\ 10^{-4}\ cm^{-1}$, $g_x = 2.001$, $g_y = 1.996$, $g_z = 1.984$. The classical ligand field theory of local $[g^{III}]$ and $[g^{IV}]$ tensors implemented with the first order perturbation theory to describe the properties of the pair does not result in a satisfying description of the $[g^{1/2}]$ tensor unless a large reduction in the spin-orbit constant is invoked. A simplified version of second-order perturbation theory leads to effects in qualitative agreement with experiment but weak as expected from the large $|J|$ value. The magnitude of these effects depends, however, on the anisotropy effects on each Mn ion. It is suggested that determination of the anisotropy of the magnetic properties of the monomeric Mn(III) and Mn(IV) moieties would be a valuable goal for a future study of these mixed valent di-manganese-di-μ-oxo complexes. The complex exhibits two quasi-reversible waves in the cyclic voltammogram, one at $E_{1/2} = 0.18$ V vs SCE for the III/IV ↔ III/III couple and the other at $E_{1/2} = 0.98$ V vs SCE for the III/IV ↔ IV/IV couple. The UV-Vis spectra of the three redox states have been recorded spectroelectrochemically.

During the last twenty years, several di-μ-oxo dimanganese complexes have been structurally characterized. There is still a continuing interest in these compounds due to their relevance to the water-oxidizing enzyme in photosystem II[1][2] and their redox catalytic properties, as shown with the mixed-valent complex $[Mn_2O_2(bpy)_4]^{3+}$[3][4][5] and its 1,10-phenantroline analogue.[4] Similar complexes using linear tetradentate ligands like *N*,*N*′-bis(2-pyridylmethyl)-1,2-diaminoethane (bispicen)[6] have been prepared in order to study their redox properties in relation to their structures.[7] We report herein the synthesis and characterization of a new dinuclear mixed-valence di-μ-oxo manganese complex with the tetradentate ligand *N*,*N*-bis(2-pyridylmethyl)-1,2-diaminoethane (*N*,*N*bispicen), an isomer of bispicen which presents a tertiary amino group as well as a primary amino group instead of the two secondary amino groups in bispicen. *N*,*N*bispicen is thus a tripodal ligand similar to tris(2-pyridylmethyl)amine (TPA)[8] and tris(2-aminoethyl)-amine (tren)[9] as shown in Scheme 1.

Scheme 1

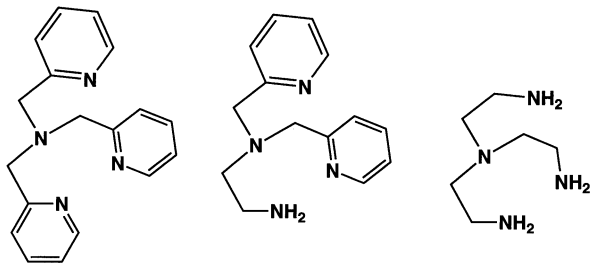

The *N*,*N*bispicen ligand has recently been used in the preparation of Fe(II) spin transition systems.[10] Unexpectedly the two primary amino groups of the two *N*,*N*bispicen ligands in the $[Mn_2O_2(N,N\text{bispicen})_2]^{3+}$ cation studied here

  1434−1948/98/0721−0727 $ 17.50+.50/0

were found in a "*cis*" configuration relatively to the Mn_2O_2 diamond core. This unusual feature gives the potential to assemble two such dimanganese complexes in a dimer of dimers.

Results and Discussion

Structure: The structure of the $[Mn_2O_2(N,N\text{bispicen})_2]^{3+}$ cation is represented in Figure 1. This cation contains a dimanganese-di-μ-oxo unit which presents no axis of symmetry. The geometry about each manganese center is approximately octahedral, with ligating atoms from the two oxo bridges and the four nitrogen atoms from the *N,N*bispicen ligand. The Mn−Mn distance is 2.646(2) Å, which is comparable to the value found in dimanganese(III,IV)-di-μ-oxo complexes previously reported.[6][8][9][11][12] The two primary amino groups from the two *N,N*bispicen ligands are situated in the same half-space delimited by the Mn_2O_2 plane. This arrangement is probably due to a combination of two different effects. Firstly, a network of hydrogen bonds can be identified involving both NH_2 groups and the two ClO_4^- anions as represented in Scheme 2.

Figure 1. ORTEP diagram of the $[Mn_2O_2(N,N\text{bispicen})_2]^{3+}$ cation with thermal ellipsoids at 50% probability; the atom labels are shown for only one chemically symmetrical part of molecule; the labeling of the Part A and Part B of molecule are similar

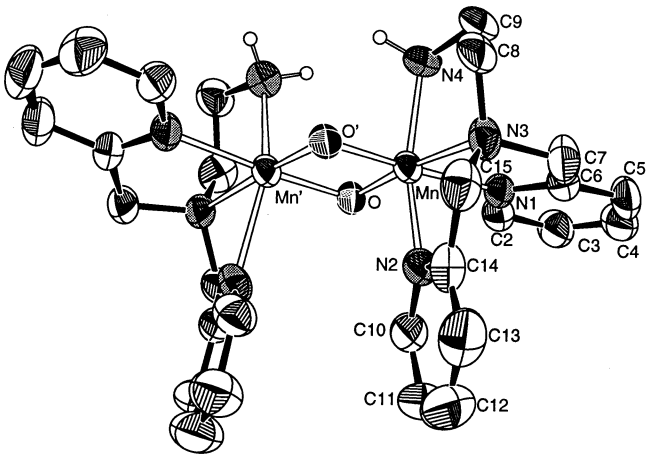

Scheme 2

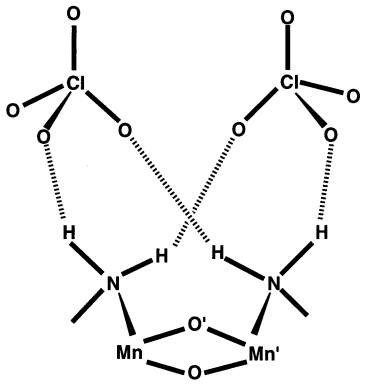

This network can be described as a cycle made of 2 Cl, 2 N, 4 O and 4 H atoms. The four distances O−N are 3.153 Å, 2.964 Å, 2.951 Å and 3.193 Å, all consistent with the presence of H bonds. Secondly a π-π interaction between the two pyridine groups appears to participate in the stabilisation of this structure. The shortest distance is that between the carbon atoms C10 and C10′ which is equal to 3.291 Å. The N2−N2′ distance is 3.412 Å.

The inequivalence between the Mn(IV) (Mn) and Mn(III) (Mn′) ions is easily recognizable from the bond distances (Table 1). The Mn equatorial pyridine distances Mn−N1 and Mn′−N′1 are, respectively 2.036(5) Å and 2.057(5) Å and the Mn-equatorial tertiary amine distances Mn−N3 and Mn′−N′3 are respectively 2.069(5) Å and 2.121(5) Å. These distances are less sensitive to the oxidation state of manganese than the axial ones. The Mn axial pyridine distances Mn−N2 and Mn′−N′2 are respectively equal to 2.015(6) Å and 2.238(6) Å and the axial Mn primary amine distances Mn−N4 and Mn′−N4′ are respectively 2.047(5) and 2.283(6) Å. This is in agreement with a $d_p^3d_{z^2}$ configuration for the Mn(III) ion (with the *z* axis perpendicular to the Mn_2O_2 plane).[12] An antibonding molecular orbital which is half occupied for the Mn(III) ion and empty for the Mn(IV) ion results fom the interaction of the d_{z^2} orbital with the σ orbitals of the axial pyridine N2 atom and the axial primary amino-group N4 atom. In previous studies it has been found that the average axial Mn(III) primary amine distance is 2.276 Å[9] in $[Mn_2O_2(tren)_2]^{3+}$ and the average axial Mn(III) pyridine distance in $[Mn_2O_2(TPA)_2]^{3+}$ is 2.233 Å.[8] These distances are similar to those found here.

Table 1. Selected bond lengths (Å) and angles (deg) for $[Mn^{III,IV}{}_2O_2(N,N\text{bispicen})_2](ClO_4)_3{\cdot}CH_3CN$

Bond lengths			
Mn−O	1.783(4)	Mn′−O	1.836(4)
Mn−O′	1.788(4)	Mn′−O′	1.838(4)
Mn−N(1)	2.036(5)	Mn′−N(1′)	2.057(5)
Mn−N(2)	2.015(6)	Mn′−N(2′)	2.238(6)
Mn−N(3)	2.069(5)	Mn′−N(3′)	2.121(5)
Mn−N(4)	2.047(5)	Mn′−N(4′)	2.283(6)
Mn···Mn′	2.646(2)		
Bond angles			
O−Mn−O′	87.6(2)	O−Mn′−N(1′)	174.7(2)
O−Mn−N(2)	96.6(2)	O′−Mn′−N(1′)	97.6(2)
O′−Mn−N(2)	95.0(2)	O−Mn′−N(3′)	96.8(2)
O−Mn−N(1)	94.7(2)	O′−Mn′−N(3′)	174.1(2)
O′−Mn−N(1)	177.2(2)	N(1′)−Mn′−N(3′)	81.6(2)
N(2)−Mn−N(1)	86.2(2)	O−Mn′−N(2′)	95.3(2)
O−Mn−N(4)	100.9(2)	O′−Mn′−N(2′)	98.9(2)
O′−Mn−N(4)	89.5(2)	N(1′)−Mn′−N(2′)	89.2(2)
N(2)−Mn−N(4)	162.0(2)	N(3′)−Mn′−N(2′)	75.3(2)
N(1)−Mn−N(4)	88.5(2)	O−Mn′−N(4′)	88.6(2)
O−Mn−N(3)	174.3(2)	O′−Mn′−N(4′)	106.7(2)
O′−Mn−N(3)	96.3(2)	N(1′)−Mn′−N(4′)	86.1(2)
N(2)−Mn−N(3)	79.0(2)	N(3′)−Mn′−N(4′)	79.1(2)
N(1)−Mn−N(3)	81.5(2)	N(2′)−Mn′−N(4′)	154.4(2)
N(4)−Mn−N(3)	83.2(2)	Mn−O−Mn′	94.0(2)
O−Mn′−O′	84.6(2)	Mn−O′−Mn′	93.7(2)

This structure can be compared in more general terms to the numerous examples already reported containing the $[Mn_2O_2]^{3+}$ core.[6][7][8][9][12][13][14] The difference between the average Mn−N(axial ligand) distances around both Mn ions reflects the asymmetry in electron distribution between the two Mn ions.[6] Here the value is 0.230 Å, which is comparable to that found for $[Mn_2O_2(bisimMe_2en)_2]^{3+}$ (0.204

Å).[12] In summary the $[Mn_2O_2(N,N\text{bispicen})_2]^{3+}$ cation is a new example of a complex of this family where the valences are profoundly differentiated.

Magnetic Susceptibility: The molar magnetic susceptibility χ_M of ground crystals of $[Mn_2O_2(N,N\text{bispicen})_2](ClO_4)_3.CH_3CN$ was measured as a function of the temperature *T*. The results are shown in Figure 2 in the form of the $\chi_M T$ versus *T* plot.

Figure 2. Product of the magnetic susceptibility per mole by temperature for $[Mn_2O_2(N,N\text{bispicen})_2](ClO_4)_3.CH_3CN$; the solid line was generated by the best fit parameters given in the text

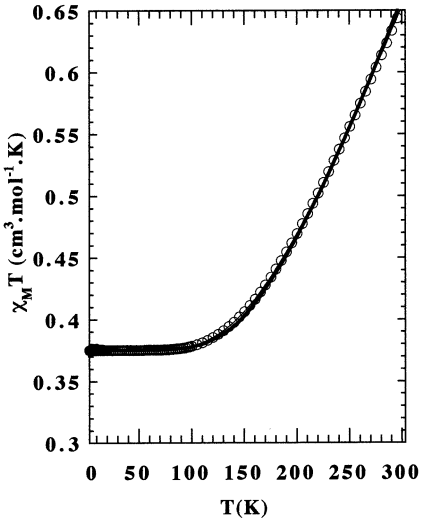

$\chi_M T$ decreases from 0.64 $cm^3mol^{-1}K$ at 292 K to a plateau at 0.38 $cm^3mol^{-1}K$ around 60 K. This is characteristic of an antiferromagnetic coupling between the electronic spins of the Mn(III) and Mn(IV) ions which produces a spin S = 1/2 ground state. This coupling is expressed by the Heisenberg hamiltonian $= -J\,\mathbf{S}_1\cdot\mathbf{S}_2$.The susceptibility was calculated according to:

$$\chi_M T = (N\beta^2 g^2/3k)(\Sigma S(S+1)(2S+1) \exp[J(S(S+1)/2kT)])/\Sigma(2S+1)\exp[J(S(S+1)/2kT)]$$

The best fit was obtained with $g = 2$ (kept constant) and $J = -316$ cm^{-1}. This value is close to that found for $[Mn_2O_2(\text{bispicMe}_2\text{en})_2](ClO_4)_3.H_2O$ ($J = -320$ cm^{-1})[11] and $[Mn_2O_2(bpy)_4](ClO_4)_3.2H_2O$ ($J = -300 \pm 14$ cm^{-1})[15] but clearly smaller than that of the strongest antiferromagnetic couplings, *J* down to -544 cm^{-1}, found in some $[Mn_2O_2L_2]^{3+}$ complexes (L representing a tetradentate ligand of the bispicen family) of ref[7], for which unfortunately no structural data is available.

EPR Spectrum: The EPR spectrum of $[Mn_2O_2(N,N\text{bispicen})_2]^{3+}$ was recorded at 10 K in acetonitrile (Figure 3a). As a first approximation this spectrum can be described as containing 16 lines, as previously observed for related complexes. Actually one may observe on closer inspection that the two lowest field lines are split. To our knowledge this feature is not generally observed in dimanganese (III,IV)-di-μ-oxo units. Another example can be found in the published spectrum of $[Mn_2O_2(TPA)_2]^{3+}$ although this was not commented upon by the authors.[16] It should be noted that the topologies of both complexes are similar. A simulation (not shown) with an axial constraint was first achieved with the following parameters: $|A_{1xy}| = 148\cdot10^{-4}$ cm^{-1}, $|A_{1z}| = 106\cdot10^{-4}$ cm^{-1}, $|A_{2xy}| = 72\cdot10^{-4}$ cm^{-1}, $|A_{2z}| = 72\cdot10^{-4}$ cm^{-1}, $g_{xy} = 1.999$, $g_z = 1.984$. The tensors were taken parallel to each other. The agreement factor *R* was found equal to 0.06. An improved simulation with $R = 0.02$, (Figure 3b) was obtained by letting the tensors become rhombic (but parallel): $|A_{1x}| = 160\cdot10^{-4}$ cm^{-1}, $|A_{1y}| = 144\cdot10^{-4}$ cm^{-1}, $|A_{1z}| = 109\cdot10^{-4}$ cm^{-1}, $|A_{2x}| = 69\cdot10^{-4}$ cm^{-1}, $|A_{2y}| = 72\cdot10^{-4}$ cm^{-1}, $|A_{2z}| = 75\cdot10^{-4}$ cm^{-1}, $g_x = 2.001$, $g_y = 1.996$, $g_z = 1.984$, $g_{iso} = 1.994$ with a line width equal to 11 G. This new set of values reproduced the splitting in the two lowest field lines mentioned above. It can be observed that the $[Mn_2O_2(tren)_2]^{3+}$ does not present this low-field feature although the ligand is also of the tripodal type. However the structure of this dimer is quite different, with the ligand bridging the two metal ions.[9]

Figure 3. X-band cw-EPR spectrum of $[Mn_2O_2(N,N\text{bispicen})_2]^{3+}$ in an 0.1 M NBu_4ClO_4 acetonitrile solution. Spectrometer setting: modulation amplitude, 1.91 G; $T = 10$ K; $\nu = 9.4384$ GHz; (a) experimental spectrum; (b) simulated spectrum

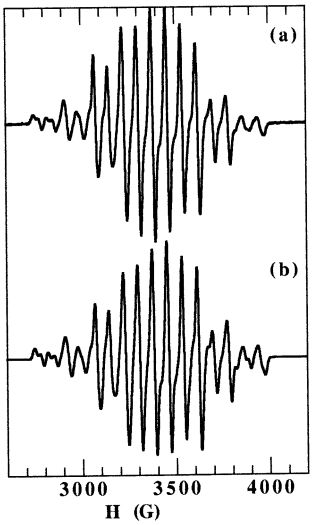

In general the spectra of the Mn(III)Mn(IV) pairs have been simulated using axial *g* and *A* tensors.[9][12][17] A rhombic simulation has been proposed for $[Mn_2O_2(bpy)_4]^{3+}$[18] (1.998, 1.992, 1.982, iso: 1.991). A ^{55}Mn ENDOR study of the same compound has used axial hyperfine tensors.[17] An X and Q band EPR and ^{55}Mn ENDOR study of $[(TACN)MnO_2(CH_3CO_2)Mn(TACN)]^{2+}$[19] has lead to rhombic tensors, in particular $g = 2.000$, 1.998, 1.984, iso: 1.994. The expression for a rhombic *g* tensor for Mn(III) has been given in ref[20]

$$\begin{aligned} g_x &= 2 - 2(\lambda/\Delta)(\cos\delta - \sqrt{3}\sin\delta)^2 \\ g_y &= 2 - 2(\lambda/\Delta)(\cos\delta + \sqrt{3}\sin\delta)^2 \\ g_z &= 2 - 8(\lambda/\Delta)(\cos\delta)^2 \end{aligned} \quad (1)$$

where λ is the spin orbit constant, Δ the energy gap between the "t_{2g}" and the "e_g"-like orbitals and δ a parameter reflecting the composition of the ground state as $|\phi> =$

$\cos\delta\ |d_{xz}d_{yz}d_{xy}d_{z^2}> + \sin\delta\ |d_{xz}d_{yz}d_{xy}d_{x^2-y^2}>$. It is also known that for the ground state of an antiferromagnetically coupled Mn(III)Mn(IV) pair one has

$$[g^{1/2}] = 2[g^{III}] - [g^{IV}] \quad (2)$$

The anisotropy of $[g^{III}]$ ($g_{perpendicular}{}^{III} = 1.990$, $g_{//}{}^{III} = 1.960$ for an elongated Mn(III) complex)[21] is larger than that of $[g^{IV}]$ ($g_{perpendicular}{}^{IV} = 1.991$, $g_{//}{}^{IV} = 1.995$ for Mn(IV) in TiO_2).[22] Initially assuming $[g^{IV}] = g^{IV}$ is isotropic, the three parameters δ, λ/Δ and g^{IV} can then be adjusted to reproduce the g values obtained. One finds $\delta = 8.14°$ ($\cos\delta = 0.9899$, $\sin\delta = 0.1416$), $\lambda/\Delta = 0.0012875$, and $g^{IV} = 1.996$. Consequently the system would be largely described by the $|d_{xz}d_{yz}d_{xy}d_{z^2}>$ wave function on Mn(III). From the type of distorsion observed in the structure it is tempting to consider the EPR z axis parallel to the axis of elongation observed in the structure. Although the g^{IV} and δ values seem reasonable, the λ/Δ ratio is smaller than expected. Indeed using $\lambda = 88\ cm^{-1}$ for the free Mn(III) ion,[20] one gets $\Delta = 68000\ cm^{-1}$ which is too large a value. This straightforward approach is thus not satisfying.

If isotropy for $[g^{IV}]$ is not assumed, the following general expression, deduced from equations 1 and 2, can be used to estimate λ/Δ.

$$g_{iso}{}^{1/2} = 4 - 8(\lambda/\Delta) - g^{IV}{}_{iso} \quad (3)$$

For instance with the value $g^{IV}{}_{iso} = 1.992$ for Mn(IV) in TiO_2[22] and $\lambda = 88\ cm^{-1}$, one finds $\Delta = 50300\ cm^{-1}$ which is still unlikely. The Δ value can be decreased by taking into account a reduction of λ reflecting covalency effects and decreasing $g^{IV}{}_{iso}$.

One may wonder if eq 2 is fully appropriate and if the extra terms due to anisotropy effects discussed by Zheng et al.[18] play a role. These terms are due to the perturbation of the spin doublet ground state by the excited spin levels. These effects have been studied for Fe(II)Fe(III) dimers in ref[23] and[24]. For the spin doublet ground state of an Mn(III)Mn(IV) pair one obtains the following modification of eq 2.

$$[g^{1/2}] = 2[g^{III}] - [g^{IV}] + (2/5)([g^{III}] - [g^{IV}])(7[D^{III}] + 2[D^{IV}])(2/-J) \quad (4)$$

Due to the large value of J, the correction introduced is expected to be small. Preliminary calculations for an elongated Mn(III) system ($\Delta g^{III} = g_{perpendicular}{}^{III} - g_{//}{}^{III} = 6\lambda/\Delta > 0$, $D^{III} < 0$) and assuming an isotropic Mn(IV) ion ($D^{IV} = 0$), show that

$$g_{iso}{}^{1/2} = 4 - 8(\lambda/\Delta) - g^{IV}{}_{iso} + (2/5)(14D^{III}/3(-J))(-2/3)(6\lambda/\Delta) \quad (5)$$

For $D^{III} < 0$, this indeed decreases the computed value for Δ by an amount proportional to D^{III} (1.6% for $D^{III} = -5\ cm^{-1}$, 3.1% for $D^{III} = -10\ cm^{-1}$). Due to the large J value as said above, this effect is weak unless the anisotropy energies be large. Nevertheless we feel that this problem has to be studied in more details for the following reasons. Little is known about the zero-field splitting energy value for Mn(III) and Mn(IV) ions in these dimers. It could well be that the zero-field splitting energy value for Mn(III) is substantial in these dimers due to a mixing of the $^3T_1$ state into the ^5E ground state of the Mn(III) ion, an effect shown recently by Caneschi et al. in a Mn(III) monomer.[21] Examination of the Tanabe-Sugano diagram for a d^4 ion shows that for a strong ligand field the $^3T_1$ state comes close to the ^5E ground state as one could sensibly predict in the case of dimers with nitrogeneous ligands. The properties of the Mn(IV) moiety also certainly deserve to be studied. In summary we propose that in order to understand in depth the electronic structure of these dimers, a better knowledge of the monomeric moieties has first to be achieved.

As for the A values, the $[A^{III}]$ presents the usual anisotropy with the lowest absolute value along the axis corresponding to the lowest g value (z) and the highest absolute principal value of the $[A^{IV}]$ tensor along the same axis.[19]

Redox Properties: The cyclic voltamogram of $[Mn_2O_2(N,N\text{bispicen})_2]^{3+}$ obtained in acetonitrile is shown in Figure 4. It shows two quasi-reversible waves, one at 0.18 V and the other at 0.98 V vs SCE. The $E_{1/2}$ value of 0.18 V corresponds to the one-electron couple III/IV $\leftrightarrow$ III/III, while that at 0.98 V represents the couple III/IV $\leftrightarrow$ IV/IV. Those two potentials are very similar to those previously reported for similar complexes with tetradentate ligands.[25]

Figure 4. Cyclic voltammetry of $[Mn_2O_2(N,N\text{bispicen})_2](ClO_4)_3.CH_3CN$ in acetonitrile, with 0.1 M $(TBA)ClO_4$ as supporting electrolyte; potentials are referenced vs SCE

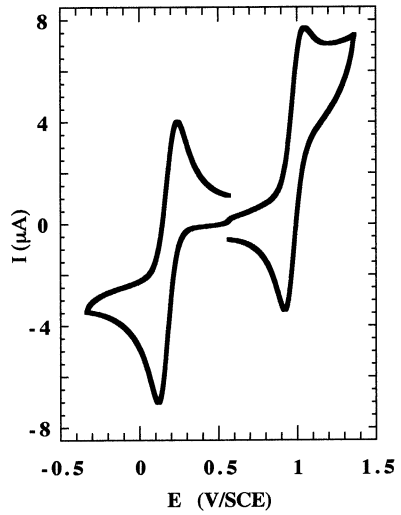

UV-Vis Spectroelectrochemistry: The spectrum of the $[Mn_2O_2(N,N\text{bispicen})_2]^{3+}$ complex as recorded in acetonitrile, is shown in Figure 5. It is comparable to those previously described for analogous dimanganese (III,IV)-di-μ-oxo units, the characteristic parameters of which have been summarized in ref[25]. It consists of a shoulder in the UV region and two bands of medium intensity in the visible region, which can be attributed as follows[26]: the 433 nm ($1080\ M^{-1}cm^{-1}$) band corresponds to a mixed contribution of Mn(IV) oxo LMCT and Mn(IV) d-d transitions, that at

Figure 5. Visible spectroelectrochemistry of the mixed-valent complex $[Mn_2O_2(N,N\text{bispicen})_2](ClO_4)_3\cdot CH_3CN$ in acetonitrile: (___) no potential applied; (–···–) oxidation at +1.14 V/SCE; (···) reduction at −0.13 V/SCE

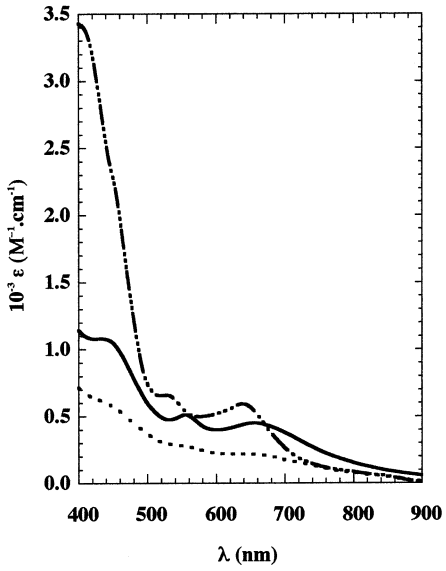

555 nm (511 $M^{-1}cm^{-1}$) to a Mn(IV) d-d transition and that at 654 nm (450 $M^{-1}cm^{-1}$) to Mn(IV) oxo LMCT.

After oxidation at +1.14 V/SCE, the spectrum of the Mn(IV)Mn(IV) form was obtained. The intensity of the absorption at 433 nm increases dramatically. This can be understood on the basis of the oxidation of the Mn(III) ion to Mn(IV). Apparently the Mn(IV) d-d band has shifted from 555 to 528 nm and its intensity has increased to 657 $M^{-1}cm^{-1}$. The band at 654 nm shifts to higher energy (637 nm) and also increases in intensity (592 $M^{-1}cm^{-1}$). This is in agreement with the attribution of such a band to an oxo Mn(IV) LMCT. After electrolysis at −0.13 V/SCE, a large decrease in the intensity of the spectrum is observed. Features at 661 (213 $M^{-1}cm^{-1}$), 556 (274 $M^{-1}cm^{-1}$) and 443 nm (595 $M^{-1}cm^{-1}$) are detected. At this potential, the Mn(III)Mn(III) form is obtained. The modifications described above are reversible by varying the potential applied appropriately. The observations reported above are very similar to those made by Brewer et al.[27] on $[Mn_2O_2(14\text{-}aneN_4)_2]^{3+}$ where 14-aneN$_4$ stands for 1,4,8,11-tetraazacyclotetradecane.

Conclusion

We have characterized a new di-μ-oxo bridged mixed valence manganese complex employing the tetradentate ligand *N,N*bispicen. The structure of the Mn(III)Mn(IV) complex has been resolved. Unexpectedly, the two primary amino groups from the two *N,N*bispicen ligands of the complex are situated on the same side of the space delimited by the Mn_2O_2 plane. Electronic, magnetic and redox properties have been reported. The EPR spectrum presents splitting of the resonances at low field which are most probably due to the rhombicity in the $[A^{III}]$ tensor. We remarked that the usual theory of the [*g*] tensor is not satisfactory unless λ is much reduced. We propose that second-order perturbation by excited spin levels on the spin doublet ground state, of the type described by Sage et al. for Fe(II)Fe(III) complexes and by Zheng et al. for Mn(III)Mn(IV), could lead to a better description if the zero-field splitting energy in those systems is important. Measurement of this energy by magnetization study and high-field EPR will be undertaken in a near future on the monomeric moieties corresponding to these dimers. The opportunity to use the two amino groups from the two *N,N*bispicen ligands in order to link two dinuclear complexes to form a tetranuclear complex will be explored.

This work has been supported in part by the *European Training and Mobility of Researchers* "Ru-Mn Artificial Photosynthesis" program (contract EU HMC network ERBXCT 94 0524).

Experimental Section

Compound Preparation: All chemical reagents were supplied by Aldrich and used without further purification. The ligand *N,N*-bis(2-pyridylmethyl)-1,2-diaminoethane (abbreviation: *N,N*bispicen) was prepared by following the procedure in ref[28]. This ligand has also recently been described in ref[10].

Caution: *Perchlorate salts of compounds containing organic ligands are potentially explosive. Only small quantities of those compounds should be prepared and handled behind suitable protective shields.*

$[Mn^{III,IV}{}_2O_2(N,N\text{bispicen})_2](ClO_4)_3\cdot CH_3CN$: 190 mg of *N,N*bispicen (0.785 mmol) were dissolved in 4 ml of absolute ethanol. To this solution 210.5 mg of $Mn(O_2CCH_3)_3.2H_2O$ (0.785 mmol) were added. After stirring for 1/2 hour, the resulting brown solution was filtered, and to the filtrate was added an absolute ethanol solution (4 ml) of $NaClO_4\cdot H_2O$ (220.5 mg, 1.57 mmol). A brown microcrystalline solid started to precipitate immediately. The solid was collected by filtration, washed thoroughly with absolute ethanol and dried under vacuum. The elemental analysis corresponds to a Mn(III)Mn(III) dimer $[Mn_2O_2(N,N\text{bispicen})_2](ClO_4)_2\cdot 1.3H_2O\cdot 1.3C_2H_5OH$. This powder was EPR silent. − $C_{30.6}H_{46.4}Cl_2Mn_2N_8O_{12.6}$: calcd C 40.43, H 5.11, Cl 7.82, Mn 12.11, N 12.33; found C 40.48, H 5.00, Cl 7.84, Mn 12.11, N 12.01. Dark single crystals characterized as $[Mn^{III,IV}{}_2O_2(N,N\text{bispicen})_2](ClO_4)_3\cdot CH_3CN$ were grown by slow diffusion of a mixture of CH_2Cl_2-$CHCl_3$ (1:1) into a concentrated solution of the powder in CH_3CN under air. − $C_{30}H_{39}Cl_3Mn_2N_9O_{14}$: calcd C 37.30, H 4.07, Cl 11.01, Mn 11.39, N 13.05; found C 37.47, H 3.94, Cl 10.95, Mn 11.38, N 13.0. − IR: $\tilde{\nu}$ = 3429 (br) cm^{-1}, 1607 (s), 1571 (w), 1480 (m), 1466(m), 1444(m), 1292 (m), 1144 (w), 1091 (vs), 766 (m), 697 (m), 660 (m), 625 (s). Symbols: br broad; vs very strong; s strong; m medium; w weak; sh shoulder. The single crystals of $[Mn^{III,IV}{}_2O_2(N,N\text{bispicen})_2](ClO_4)_3\cdot CH_3CN$ were used for all subsequent physical measurements.

Electrochemical Measurements: Cyclic voltammetry was measured using a EGG PAR potentiostat (M 273 model). The working electrode was a Pt disk of 3 mm diameter, carefully polished with diamond pastes and ultrasonically rinsed in ethanol before use. A Pt wire was used as counter electrode and as reference, a Ag/$AgClO_4$ electrode, prepared in acetonitrile and separated by a fritted disk from the main solution (270 mV above the potential of the saturated calomel electrode). The experiment was carried out on a carefully degassed solution by argon flushing.

Magnetic Susceptibility Measurements: Magnetic susceptibility measurements in the 4.2−300 K temperature range were carried

out with a MPMS5 SQUID magnetometer (Qantum Design Inc.). The calibration was made at 298K using palladium reference sample furnished by Quantum Design Inc. Ground crystals of $[Mn^{III,IV}_2O_2(N,N\text{bispicen})_2](ClO_4)_3.CH_3CN$ were used.

Crystallographic Data Collection and Refinement of the Structure of $[Mn^{III,IV}_2O_2(N,N\text{bispicen})_2](ClO_4)_3\cdot CH_3CN$: The crystal data of $[Mn^{III,IV}_2O_2(N,N\text{bispicen})_2](ClO_4)_3\cdot CH_3CN$ and the parameters of data collection are summarized in Table 2. A prismatic black crystal with the dimensions 0.9 × 0.25 × 0.15 mm was mounted in a glass capillary with 0.5 mm diameter. The unit-cell and intensity data were measured with an Enraf-Nonius CAD-4 diffractometer with graphite monochromated Mo-K_α radiation (λ = 0.71073 Å). The cell constants were obtained by least-squares procedures based upon the 2Θ values of 25 reflections measured in the ranges $20.8° < 2\Theta < 21.6°$ at ambient temperature. All reflection intensities were collected in the range $4° < 2\Theta < 50°$ within [$-19 \le h \le 19$, $-13 \le k \le 13$, $0 \le l \le 29$]. The total number of the collected and independent reflections are 16114 and 7870. Due to the peculiar form of the single crystal an empirical absorption correction was carried out. The structure was solved by direct methods with the program SHELXS86[29] and refined by using the SHELXL93[30] programs. The figure was prepared with ORTEP II.[31] The molecular cation was located in a general crystallographic position as well as three perchlorate anions and the molecule of acetonitrile. Observed disorder in the stucture involved the anions; all were disordered over two sites with non-identical occupations (0.60 and 0.40). The stucture was refined by full-matrix least-squares approximation based on F^2. Refinement was anisotropic for non-H atoms. Hydrogen positions were calculated by assuming geometrical positions and were included in the structural model (In addition, a cluster of electron density with seven different peak positions was found and these were not identified). Final refinement of this model was continued until convergence when $R1$ = 0.066 for $F^2 > 2\sigma(F^2)$ and R_w = 0.242. The final difference map showed two largest residual peaks of 0.68 and −0.66 eÅ^{-3}. Crystallographic data (excluding structure factors) for the structure reported in this paper have been deposited with the Cambridge Crystallographic Data Centre as supplementary publication no. CCDC-100897. Copies of the data can be obtained free of charge on application to The Director, CCDC, 12 Union Road, Cambridge CB2 1EZ, UK [Fax: (int. Code) +44(1223)336-033, E-mail: deposit@chemcrys.cam.ac.uk, World Wide Web: http://www.ccdc.cam.ac.uk].

Table 2. Crystallographic data for $[Mn^{III,IV}_2O_2(N,N\text{bispicen})_2](ClO_4)_3 \cdot CH_3CN$

Formula	$Mn_2C_{28}H_{36}N_8Cl_3O_{14}\cdot CH_3CN$
fw	965.93
Radiation	Mo-K_α (0.71073 Å)
Temp (K)	293
Space group	*P*21/*c*
a (Å)	16.511(9)
b (Å)	11.113(5)
c (Å)	24.55(2)
α (deg)	90
β (deg)	91.33(8)
γ (deg)	90
V (Å^3)	4503(5)
Z	4
μ (mm^{-1})	0.818
N_{meas}	16114
N_{obs}	7870
R	0.066
R_w	0.242

EPR Spectroscopy: EPR spectrum was recorded on Bruker ER 200 D spectrometer at X-band. For low temperature studies, an Oxford Instruments continuous flow liquid helium cryostat and a temperature control system were used. In order to get a good quality glass a 0.1 M solution of NBu_4ClO_4 in acetonitrile was used as solvent.

EPR Simulation: Simulation of the EPR spectrum was performed using a FORTRAN program originally developed by Drs L. K. White and R. L. Belford at University of Illinois. The program simulates powder spectra for S = 1/2 systems and can include four different hyperfine interactions using perturbation theory. It was modified to allow for calculation of the hyperfine contributions to the spectra to the second order.[32] Briefly, for each transition, the resonant field was calculated using perturbation theory up to the second order for the hyperfine coupling terms and the resulting stick spectrum was then convolved with Gaussian functions. This simulation program is coupled to a minimization program in order to find the set of parameters giving the lowest possible value of the agreement factor defined as $R = \Sigma_i(Y_i^{calc} - Y_i^{exp})^2/\Sigma_i Y_i^{exp\ 2}$.

[1] V. K. Yachandra, K. Sauer, M. P. Klein, *Chem. Rev.* **1996**, *96*, 2927−2950.
[2] W. Rüttinger, G. C. Dismukes, *Chem. Rev* . **1997**, *97*, 1−24.
[3] Abbreviations used: bispicMe$_2$en = *N*,*N*′-dimethyl-*N*,*N*′-bis(2-pyridylmethyl)ethane-1,2-diamine; bpy = 2,2′-bipyridine; bisimMe$_2$en = *N*,*N*′-Dimethyl-*N*,*N*′-bis(imidazol-4-ylmethyl)ethane-1,2-diamine); *N*,*N*bispicen = *N*,*N*-bis(2-pyridylmethyl)-1,2-diaminoethane; TPA = tris(2-pyridylmethyl)amine; tren = tris(2-aminoethyl)amine.
[4] S. R. Cooper, M. Calvin, *J. Am. Chem. Soc.* **1977**, *99*, 6623−6630.
[5] A. Gref, G. Balavoine, H. Riviere, C. P. Andrieux, *Nou. J. Chim.* **1984**, *8*, 615−618.
[6] M. A. Collins, D. J. Hodgson, K. Michelsen, D. K. Towle, *J. Chem. Soc., Chem. Commun.* **1987**, 1659−1660.
[7] P. A. Goodson, J. Glerup, D. J. Hodgson, K. Michelsen, H. Weihe, *Inorg. Chem* . **1991**, *30*, 4909−4914.
[8] D. K. Towle, C. A. Botsford, D. J. Hodgson, *Inorg. Chim. Acta* **1988**, *141*, 167−168.
[9] K. S. Hagen, W. H. Armstrong, H. Hope, *Inorg. Chem.* **1988**, *27*, 967−969.
[10] G. S. Matouzenko, A. Bousseksou, S. Lecocq, P. J. van Koningsbruggen, M. Perrin, O. Kahn, A. Collet, *Inorg. Chem.* **1997**, *36*, 2975−2981.
[11] J. Glerup, P. A. Goodson, A. Hazell, R. Hazell, D. J. Hodgson, C. J. Mc Kenzie, K. Michelsen, U. Rychlewska, H. Toflund, *Inorg. Chem* . **1994**, *33*, 4105−4111.
[12] Y.-M Frapart, A. Boussac, R. Albach, E. Anxolabéhère-Mallart, M. Delroisse, J.-B. Verlhac, G. Blondin, J.-J. Girerd, J. Guilhem, M. Cesario; A. W. Rutherford, D. Lexa, *J. Am. Chem. Soc.* **1996**, *118*, 2669−2678.
[13] P. M. Plaskin, R. C. Stoufer, M. Mathew, G. J. Palenik, *J. Am. Chem. Soc* . **1972**, *94*, 2121−2122.
[14] M. Stebler, A. Ludi, H.-B. Bürgi, *Inorg. Chem.* **1986**, *25*, 4743−4750.
[15] S. R. Cooper, G. C. Dismukes, M. P. Klein, M. Calvin, *J. Am. Chem. Soc.* **1978**, *100*, 7248−7252.
[16] X.-L Tan, Y. Gultneh, J. Sarneski, C. P. Scholes, *J. Am. Chem. Soc.* **1991**, *113*, 7853−7858.
[17] D. W. Randall, B. E. Sturgeon, J. A. Ball, G. A. Lorigan, M. K. Chan, M. P. Klein, W. H. Armstrong, R. D. Britt, *J. Am. Chem. Soc.* **1995**, *110*, 11780−11789.
[18] M. Zheng, S. V. Khangulov, G. C. Dismukes, V. V. Barynin, *Inorg. Chem.* **1994**, *33*, 382−387.
[19] W. Zweygart, R. Bittl, K. Wieghardt, W. Lubbitz, W. *Chem. Phys. Letters*, **1996**, *261*, 272−276.
[20] A. Abragam, B. Bleaney, *Electron Paramagnetic Resonance of Transition Ions,* Oxford University Press **1970**.
[21] A. Caneschi, D. Gatteschi, R. Sessoli, *J. Chem. Soc. Dalton Trans.* **1997**, 3963−3970. A.-L. Barra, D. Gatteschi, R. Sessoli, G. L. Abbati, A. Cornia, A. C. Fabretti, M. G. Uytterhoeven, *Angew. Chem. Int. Ed. Engl.* **1997**, *36*, 2329−2331.
[22] H. G. Andresen, *Phys. Rev.* **1961**, *35*, 1090−1096.

[23] J. T. Sage, Y. M. Xia, P. G. Debrunner, D. T. Keough, J. de Jersey, B. Zerner, *J. Am. Chem. Soc.* **1989**, *111*, 7239−7247.
[24] B. Guigliarelli, P. Bertrand, J.-P. Gayda, *J. Chem. Phys.* **1986**, *85*, 1689−1692.
[25] P. A. Goodson, J. Glerup, D. J. Hodgson, K. Michelsen, E. Pedersen, *Inorg. Chem* . **1990**, *29*, 503−508.
[26] D. R. Gamelin, M. L. Kirk, T. L. Stemmler, S. Pal, W. H. Armstrong, J. E. Penner-Hahn, E. I. Solomon, *J. Am. Chem. Soc.* **1994**, *116,* 2392−2399.
[27] K. J. Brewer, M. Calvin, R. S. Lumpkin, J. W. Otvos, L. O. Spreer, *Inorg. Chem.* **1989**, *28*, 4446−4451.
[28] O. Horner, E. Anxolabéhère-Mallart, M. F. Charlot, L. Tchertanov, J. Guilhem, A. Boussac, J.-J. Girerd, submitted for publication.
[29] G. M. Sheldrick, *SHELXS86, Program for Crystal Structure Solution;* University of Göttingen, Germany, **1986**.
[30] G. M. Sheldrick, *SHELXL93, Program for Crystal Structure Solution*; University of Göttigen, Germany, **1993**.
[31] C. K. Johnson, *ORTEPII.* Report ORNL-5138. Oak Ridge National Laboratory, Tennessee, USA., **1976**
[32] J. Bonvoisin, G. Blondin, J.-J. Girerd and J.-L. Zimmermann, *Biophys. J.* **1992**, *61*, 1076−1086.

[97299]